Petroleum & Coal
ISSN 1337-7027

Available online at www.vurup.sk/petroleum-coal
Petroleum & Coal 57(5) 447-465, 2015

MODELING OF RHEOLOGICAL PROPERTIES OF CLASS G CEMENT SLURRY

K. K. Salam*, A. O. Arinkoola, B. M. Ajagbe, and O. Sanni

*Petroleum Engineering Unit, Department of Chemical Engineering, Ladoke Akintola University of Technology, Ogbomoso.*Corresponding author: kaykaysalam@yahoo.co.uk*

Received December 10, 2014, Revised October 6, 2015, Accepted October 12, 2015

Abstract

The role of rheology is important during cement slurries design because it directly affect the quality of primary cementing in the area of determination of the relationship of pressure to depth during and after repression, return circulation to calculate the phase of "free fall", forecasts temperature profile during pumping a cement slurry design and capacity required for optimal suppression of cement puree. With the aid of design of experiment three different regression models were developed for plastic viscosity (PV), apparent viscosity (AP) and yield point (YP) for class G cement slurry subject to behavior of four different variables extender (A), accelerator (B), antifoam (C) and dispersant (D). A full factorial design at two level was used to analyze sixteen experimental run replicated twice. The analysis was done with design expert 6.08. The regression equations developed for plastic viscosity, apparent viscosity and yield point established important parameters that affect the rheology properties with correlation coefficient of 0.9939, 0.9543 and 0.9574 with corresponding standard error of 0.098, 0.00437 and 0.3 respectively.

Keywords:

1. Introduction

The role played by rheology during cement slurry design are in assuring that the cement slurry can be mixed at the surface and pumped into the well at minimum pressure drop; in governing the flow regime for optimum cement slurry placement and in maintaining the solid particle in suspension during the fluid state of cement slurry [1]. These made cement slurries to be important in the design, construction and quality of primary cementing which aid in determination of the relationship of pressure to depth during and after repression, return circulation to calculate the phase of "free fall", forecasts temperature profile during pumping a cement slurry design and capacity required for optimal suppression of cement puree [2].

Presence of additives with different chemical compositions for different purposes in the cement mixture influenced the rheological behavior of cement slurries and to control major properties of cement properties like thickening time, consistency, fluid-loss rate, free water, setting time, strength development of cement stone to the pressure, density, and the possibility of mixing special requirements (gas migration control, thixotropy, expansion, strong bonds with protection pipe and formation) *etc*. [3]. Consequently, a wide variety of cement additives is now available to alter cement properties to meet most well conditions [4]. Arild *et al.* [5] investigated the effect of addition of different quantities of gypsum and anhydrite on rheological properties of cement slurries at different temperature. The result was concluded that substitution of gypsum with anhydrite positively affect the rheological properties of cement slurry and also that the temperature effect on the rheological properties was dependent on different ratio of gypsum/anhydrite in the cement slurry

In order to prevent cement strength retrogression Helge *et al.* [6] investigated effect of different type of additives that control strength regression under high temperature condition

on rheological properties of cement slurry. Class G cement and cement partly replaced by silica were the two cement materials used in preparing eight different cement slurries with different variations in their additivities. When cement was partly replaced by silica flour and the water content was adjusted to maintain the same slurry density the slurry viscosity is increased. For dispersant and retarder free slurries the addition of liquid micro silica leads to an increase in viscosity. If the investigated retarder and dispersant are present the viscosity was reduced by addition of liquid micro silica. Above situation was also observed in the work of Roni *et al.* [1] who investigated the implication of rheological properties on sedimentation phenomenon of class G cement.

Gonet *et al.* [7] analysed the complex character that guide rheological investigation by using published equations describing rheological models to validate experimental results for three different cement slurries. The selected cement slurries were analysed in laboratory conditions for various water-cement ratio from 0.4 to 1.2 for three different cement types, three different temperatures 278, 293 and 323 K of the cement slurry and appropriate rheological model from the three popularly used rheological models Bingham's, Ostwald de Waele's and Casson's model that suite prediction. The obtained results were statistically analysed and the best fit of the rheological model to the individual cement slurries was selected. Bingham's model is most frequent for water-to-cement ratios ranging between 0.8 and 1.2, Ostwald de Waele's model described cement slurries made in temperatures between 293 and 323 K and Casson's model much better describes cement slurries based on lower water-to-cement ratios (0.4 to 0.8)

Gintautas *et al.* [8] investigated the influence of shapes of two different cement types on behaviour of their rheological properties of the two selected cement types. Portland cement particles shape and concentration on yield stresses, viscosity and dilatancy of Portland cement and Ground Granulated Blast furnace Slag (GGBS) cement slurries. Portland cement predominantly has particles of spherical shape while GGBS particles are characterized by sharp edges and angles, the cement slurry are designed for a water-cement ratio between 0.55 to 0.80. The results from the investigation show that yield stress and viscosity of GGBS cement slurry increases about 2 times more than this of the slurry of Portland cement with increase in water-cement ratio while yield stress and viscosity decreased with increased in water-cement ratio. The changes of the cement slurry viscosity and yield stress could be described by exponential equation, which must be modified with the two coefficients in Mooney equation depending on the particles shape and particle volume distribution density for accuracy of the equation. Also the use of materials for alternating the compressive strength of cement in the work of Ershadi *et al.* [9] who used nanosilica to improve slurry impermeability of gas intrusion into cement by Improving rheological and mechanical properties of cement slurry. The result of the work showed that increase in nanosilica improved rheological properties and decreased the density of the cement slurry.

In order to account for pressure loss as a result of neglect of consistency in rheological investigation, Pattinasarany and Irawan [9] developed a new model that can determine the effect of cement slurry consistency toward viscosity and friction pressure. Classes G cement slurry rheological readings were taking at different time from 0 to 80 using five different dial readings. The result was used to fit power law flow consistency index and validated using correlation coefficient. Friction pressure was calculated for three different components. It was observed from the that when rheological investigation was determined at different thickening time from 0 to 80min lead increase in consistency with increase in thickening time which leads to about 129% increase in friction pressure when compared with pressure drop without effect of consistency.

Dale *et al.* [10] designed experiments used to investigate the influence of three variables cement particle size distribution (PSD), fly ash PSD, and ratio of fly ash to cement at four levels on the yield stress and viscosity of blended pastes. Both rheological parameters are seen to vary over several orders of magnitude for the evaluated design space. It was observed that at constant solid volume fraction the replacement of cement by fly ash decreased the

yield stress and increased in the value plastic viscosity which is attributed to higher surface area of the slurry. This suggested that for the plastic viscosity of a flowing system, both the cement and the fly ash particles are contributing to the measured increase relative to the value for the solution itself, in contrast to the yield stress, which was dominated by the properties of the cement particles.

For a desired slurry design, extensive laboratory examination of the various parameters is required and in most cases it may be extremely difficult or impossible to meet all the slurry properties that would be considered ideal. The accurate and reliable characterization of cement slurries still presents a problem for the industry [12]. Factorial Design is a tool that can simultaneously monitor interactions of multiple factors which accommodate the effect of both main and interaction effects [13] which has been successfully used to solve some engineering problems. Salam *et al.*, [14] established the relationship among three variables that affect wax deposition along pipeline based on experimental results reported by Kelechukwu *et al* [15]. Also Falode *et al.* [16] and Salam *et al.* [17] applied Yates algorithm using Factorial design to predict a model that study interaction of four factors on compressive strength and thickening time of class G cement slurry.

Anjuman and Moncef [4] with the aid of Artificial Neural Network (ANN) and Multiple Regression Analysis (MRA) developed two separate models that can predict shear stress of class G cement as a function of three variables temperature, admixture dosage and shear rate mixed with three different additives polycarboxylate-based high-range water reducing admixture (PCH), polycarboxylate-based mid-range water reducing admixture (PCM), and lignosulphonate-based mid-range water reducing admixture (LSM) were the water reducing additives added to the cement slurry with water-cement ratio of 0.44 under different temperature with a range of 23 to 60ºC. The models developed by both approaches were found to be sensitive to the effects of temperature increase and admixture dosage on the rheological properties of oil well cement (OWC) slurries. While the ANN-based model performed relatively better than the MRA-based model in predicting the rheological properties of OWC slurries. The interactions among various additives play a vital role in altering the rheological properties of OWC slurries and in most cases it may be extremely difficult or impossible to meet all the slurry properties This study will implement a mathematical model to predict plastic viscosity, apparent viscosity and yield point using design expert 6.08 subject to four different variables that will be used to study interaction among selected additives for a class G cement slurry.

2. Methodology

Slurry preparation was reported in our earlier work on Salam *et al.* [17] and Falode *et al.* [16]. The samples were prepared based on the full factorial design reported in sited journals above and tabulated in Table 1.

Table 1 Experimental design for two levels

S/No	A	B	C	D	S/No	A	B	C	D
1	1	1	-1	1	9	1	-1	-1	-1
2	1	-1	1	-1	10	-1	-1	-1	-1
3	-1	1	-1	-1	11	1	1	-1	-1
4	-1	-1	1	-1	12	-1	1	1	1
5	1	-1	-1	1	13	1	1	1	1
6	-1	1	1	-1	14	-1	-1	1	1
7	1	1	1	-1	15	-1	1	-1	1
8	-1	-1	-1	1	16	1	-1	1	1

Sixteen experimental runs were prepared based on the table presented and rheological parameters were determined for each of the sixteen runs. The slurries were prepared using

a variable speed high-shear blender type mixer with bottom drive blades as per the API Recommended Practice 10B-2 [18]. The variables are named as: A – Extender, B – Accelerator, C – Antifoam and D – Dispersant respectively. The Bingham model was used throughout this study to calculate the rheological properties of cement slurries, i.e. yield stress and plastic viscosity and apparent viscosity. Cement slurries shear were measured at 600rpm and 300rpm using rotational viscometer with coaxial cylinders BCH-3. The shears values were used to determine the Bingham model parameters using the formular presented in the work of Adeleye *et al.* [19].

2.1 Model development

The model equation like the one expressed in equation 2 will be developed for the prediction of apparent viscosity, plastic viscosity and yield point based on design of experiment in Table 2. The full factorial design for the experiment was run twice. Multiple regression analysis was used to correlate the responses of apparent viscosity, plastic viscosity and yield point with the four different variables studied. Apparent viscosity, plastic viscosity and yield points were calculated using the formular in the work of Adeleye *et al.* [19].

$$Y = \beta_0 + \beta_A A + \beta_B B + \beta_C C + \beta_D D + \beta_{AB} AB + \beta_{AC} AC + \beta_{AD} AD + \beta_{BC} BC + \beta_{BD} BD + \beta_{CD} CD + \beta_{ABC} ABC + \beta_{ABD} ABD + \beta_{ACD} ACD + \beta_{BCD} BCD + \beta_{ABCD} ABCD \quad (2)$$

Table 2 Variable level settings

Factors	Levels		
	Low (-1)	Mid-point (0)	High (+1)
A	5	10	15
B	0	5	10
C	0	3.95	7.9
D	0	2.1	4.2

3. Results and discussion

3.1 Regression model equation for the apparent viscosity/model fitting

The model equation developed for the prediction of rheological properties of class G cement slurry and factors interaction are presented in this section. The result of the factorial design in actual values for the model development run twice was presented in Table 3 and equation developed for each of the rheological properties was expressed in equation 4 -6.

$$A_v = 15.59 + 1.09A + 1.75B + 0.72C + 2.41D - 1.81AB - 1.34AC - 2.28AD - 2.62BC - 0.94BD - 2.47CD + 3.13ABC + 0.44ABD + 1.66ACD + 0.94BCD \quad (4)$$

$$(P_v)^{-1} = 0.173313 - 0.02269A - 0.02996B - 0.01964C + 0.001314D + 0.02443AB + 0.040451AC + 0.011062AD + 0.030208BC + 0.003051BD + 0.016195CD - 0.02468ABC + 0.001984ABD - 0.00503BCD \quad (5)$$

$$Y_p = 21.25 - 1.75A + 0.31B - 0.75C + 2.63D - 1.06AB + 1.37AC - 1.5AD - 0.69BC + 0.69BD - 1.38CD + 2.31ABC - 1.06ABD + 0.88ACD - 0.81BCD + 2.06ABCD \quad (6)$$

Table 3 Results from the experimental design

S/No	A	B	C	D	A_V	P_V	Y_P
1	15	10	7.9	4.2	16	5	22
2	15	0	7.9	0	17	7	20
3	5	10	7.9	0	14	4	21
4	5	10	0	0	15.5	6	19
5	5	0	7.9	4.2	20	8	24
6	15	10	0	4.2	16.5	8	17
7	5	0	0	0	13	4	19
8	15	0	7.9	4.2	15	5	20
9	15	0	0	4.2	20	7	26
10	5	0	7.9	0	18	8	20
11	5	10	7.9	4.2	15	6	18
12	5	10	0	4.2	28.5	9	39
13	5	0	0	4.2	14	3	22
14	15	10	0	0	17.5	10	15
15	15	0	0	0	16	7	18
16	15	10	7.9	0	17	7	20
17	15	0	7.9	0	16.5	7	19
18	5	10	0	4.2	28	7	42
19	15	0	7.9	4.2	14	5	18
20	15	10	7.9	4.2	16.5	5	23
21	15	10	0	0	17	8	18
22	15	10	7.9	0	16.5	7	19
23	15	10	0	4.2	16	8	16
24	5	0	0	0	12.5	3	19
25	15	0	0	4.2	20.5	9	23
26	5	10	0	0	15	6	18
27	5	10	7.9	4.2	14	9	22
28	5	0	7.9	0	17.5	8	19
29	5	10	7.9	0	14.5	5	16
30	15	0	0	0	15	6	18
31	5	0	0	4.2	14.5	3	23
32	5	0	7.9	4.2	19.5	6	27

3.1.1 Interaction of variables on apparent viscosity

Shown in Figure 1(i-iv) are the individual behavior of the four factors used for the prediction of apparent viscosity. Figure 1(i) show that at constant accelerator of 5%, antifoam of 3.95% and dispersant of 2.10%; the relationship between the apparent viscosity and extender was a proportional relationship. There was an increase in the value of apparent viscosity from 14 to 16.6875 when the percentage of extender was increased from 5 to 15%.

Figure 1(ii) show that the relationship between the apparent viscosity and accelerator was a proportional relationship with constant percentages of extender , antifoam and dispersant, respectively. There was an increase in values of apparent viscosity from 13.8437 to 17.3438 when the percentage of accelerator was increased from 0 to 10%. Presented in Figure 1(iii)

was the inverse relationship between apparent viscosity and antifoam at constant extender, accelerator and dispersant. There was an increase in value of apparent viscosity of class G cement slurry from 14.875 to 16.3125 when the percentage of antifoam was varied from 0 to 7.9. Figure 1(iv) also showed a proportional relationship between the apparent viscosity and dispersant at constant extender, accelerator and antifoam. There was an increase in the value of apparent viscosity from 13.1875 to 18 when the dispersant percentage was increased from 0 to 4.2%.

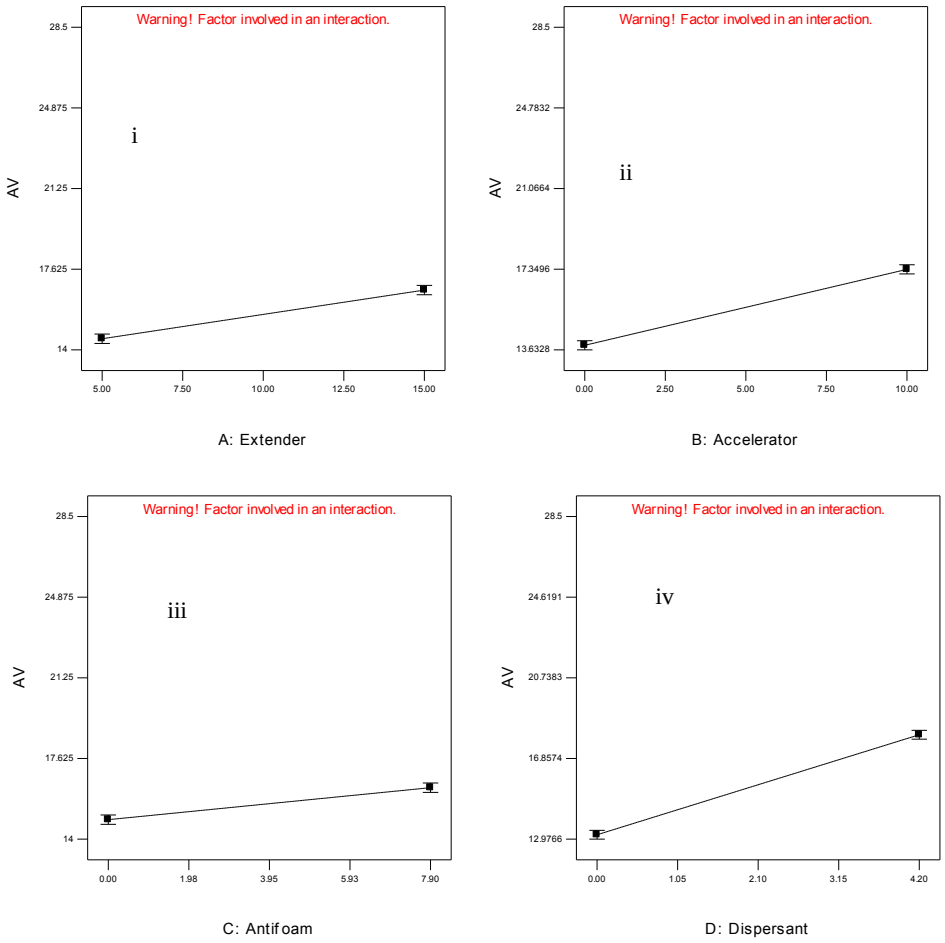

Figure 1: Effect of individual variable on Apparent Viscosity

Figure 2(i-vi) show different combinations and effects of combining two variables and keeping other variables constant on apparent viscosity. Figure 2(i) show the effect of low and high values of accelerator with increase in extender percent from 5 to 15% at constant antifoam and dispersant. It was observed that at a low value of accelerator, the apparent viscosity increased from 10.9375 to 15 when extender value was increased from 5 to 15%, and increasing the value of accelerator to 10, the apparent viscosity decreased from 18.0625 to 16.625 when the extender value was increased from 5 to 15%. Figure 2(ii) showed the effect of simultaneous increase in value of extender and antifoam on apparent viscosity at constant accelerator and dispersant. It was noticed that increase in extender from 5 to 15% led to increase in apparent viscosity from 12.4375 to 17.3125 at a low antifoam value and at a high antifoam value of 7.9%, the apparent viscosity slightly decreased from 16.5625 to 16.0625 when the extender value was increased from 5 to 15%. Different behavior was noticed for different combinations of two factors variables of extender and dispersant, accelerator and

antifoam, accelerator and dispersant and antifoam and dispersant which are all pictorially represented in Figure 2(iii-vi).

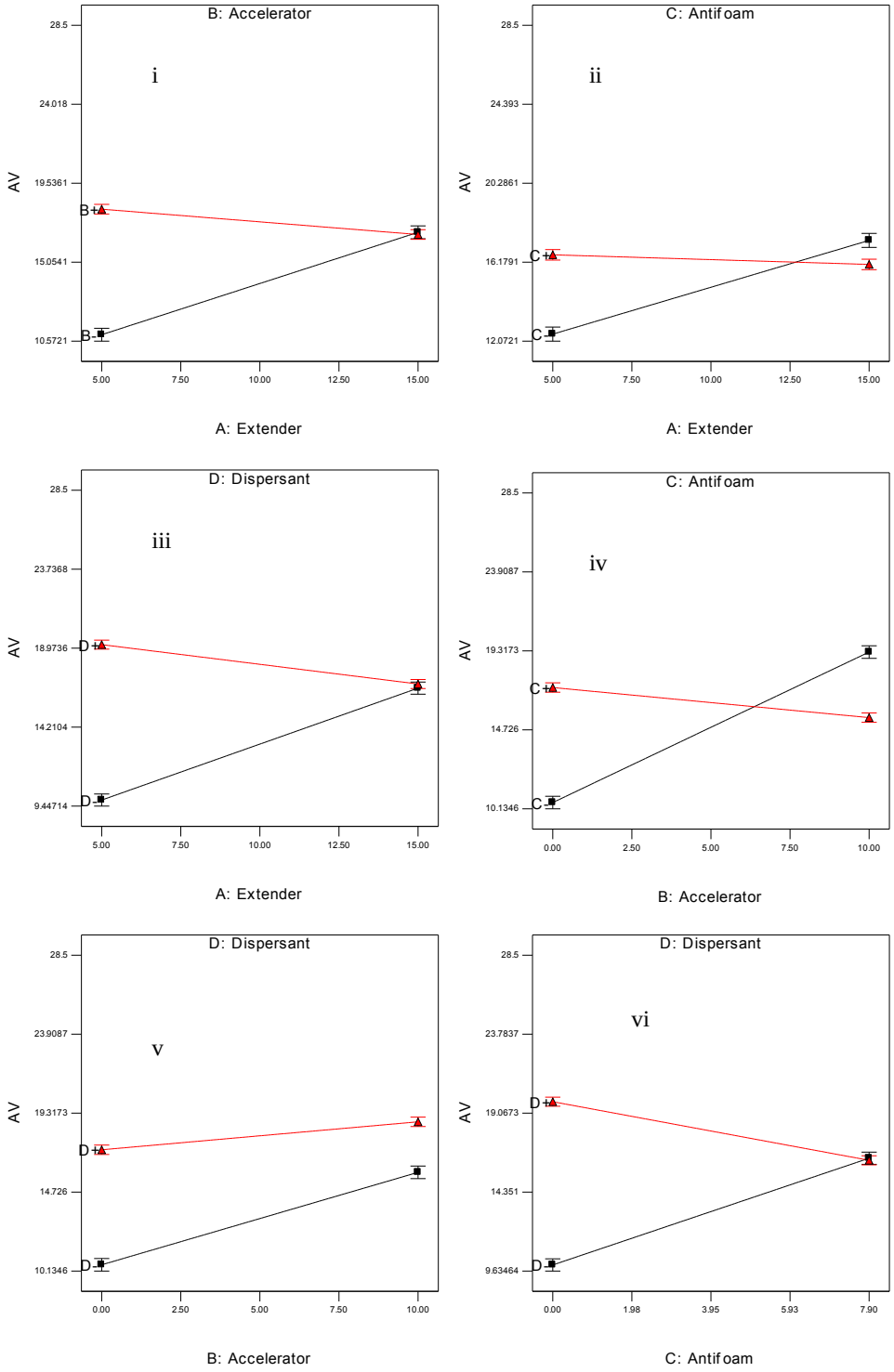

Fig 2: Effect of interactions of variables on Apparent viscosity

Figure 3(i-vi) described the surface behavior of combination of variables on response variable.

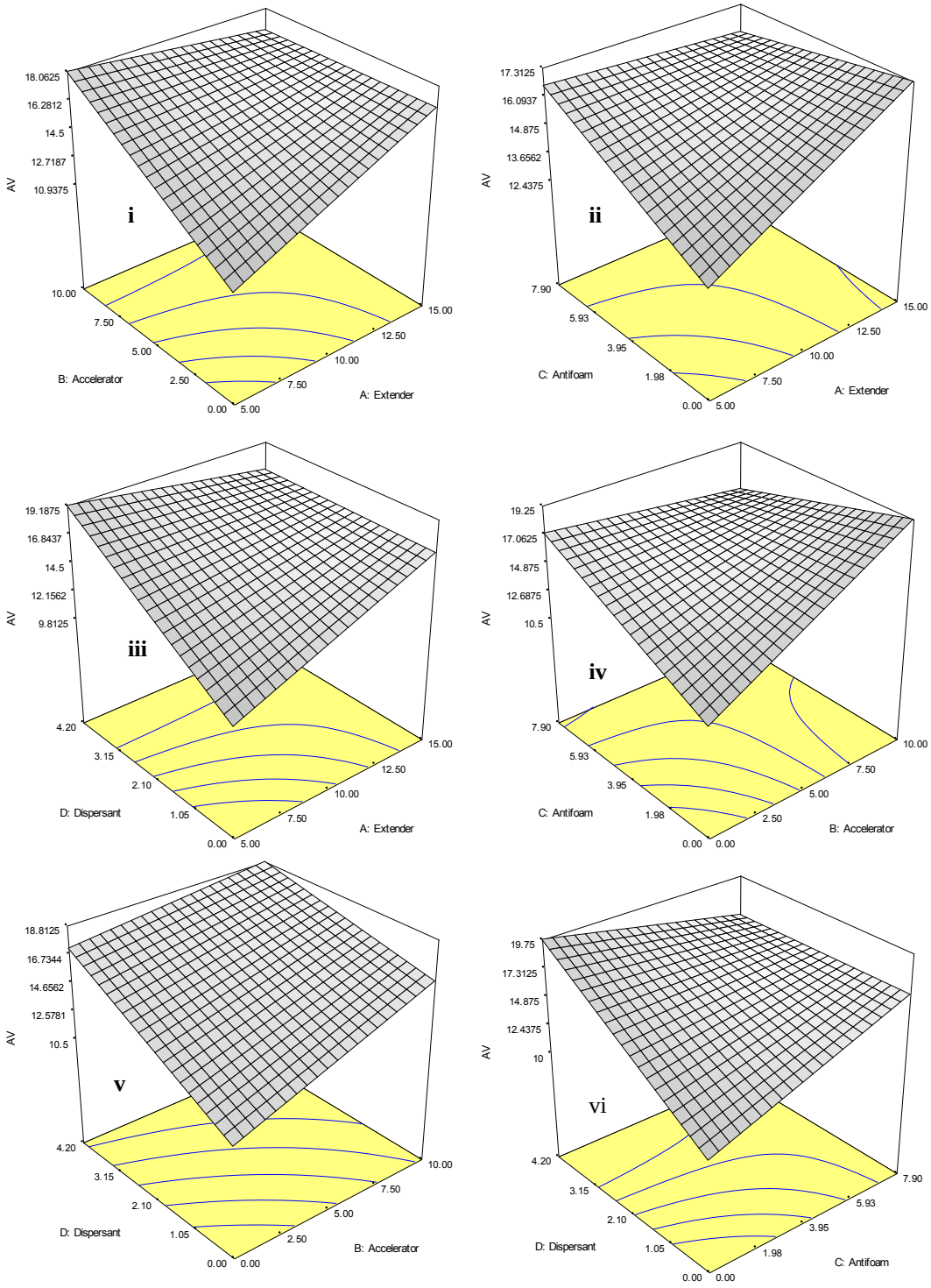

Fig 3: Surface plot of variables against AV

Figure 3i show the 3D view of surface interaction between extender and accelerator at constant antifoam and dispersant. The surface plot show that apparent viscosity increased from 10.9375 to 15 when the extender value was increased, increase in antifoam value to 7.9 led to

increase in apparent viscosity given a maximum value of 18.0625 at extender value of 5% and further increase in extender value led to decreased in the apparent viscosity with a value of 16.625 at 15%. Figure 3(ii) show the 3D surface interaction of extender and antifoam at constant accelerator and dispersant. It was observed that at low antifoam and high value of extender highest value of apparent viscosity was recorder as 17.3125. Increase in value of antifoam increased the value of apparent viscosity from 12.4375 to 16.5625 at a minimum value of extender but increased in extender value at high antifoam percent tend to have a detrimental effect to apparent viscosity increment with a value of 16.8125 at 15%. Surface interaction of extender and dispersant at constant accelerator and antifoam was shown in Figure 3(iii). It was observed from the plot that at a high dispersant value of 4.2%, a very high value of apparent viscosity of 19.1875 was recorded at extender value of 5% but increase in the exten-der value drastically increased apparent viscosity value to 16.8125 at 15% while in the absence of dispersant apparent viscosity value increased from 9.8125 to 16.5625 when extender value was increased from 5 to 15%. 3D plot for accelerator - antifoam, accelerator - dispersant and antifoam - dispersant were all presented in Figure 4(iv-vi).

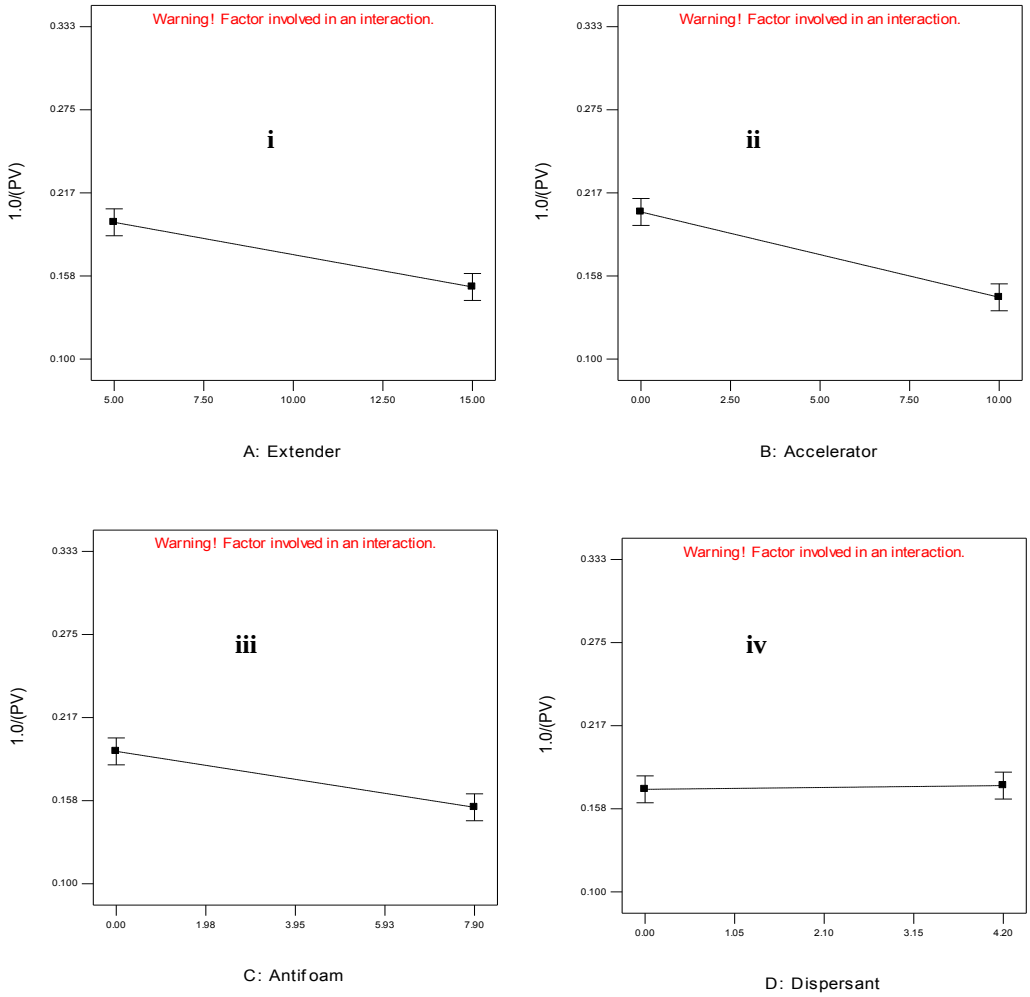

Fig 4: Effect of each variable on PV

3.1.2 Interaction of variables on plastic viscosity

Figure 4(i-iv) show individual behavior of the four factors used for the prediction of plastic viscosity. Figure 4(i) show that at constant accelerator of 5%, antifoam of 3.95% and dispersant

of 2.10%; the relationship between the plastic viscosity and extender was an inverse relationship. There was a decrease in the value of plastic viscosity from 0.196 to 0.151 when the percentage of extender was increased from 5 to 15%.

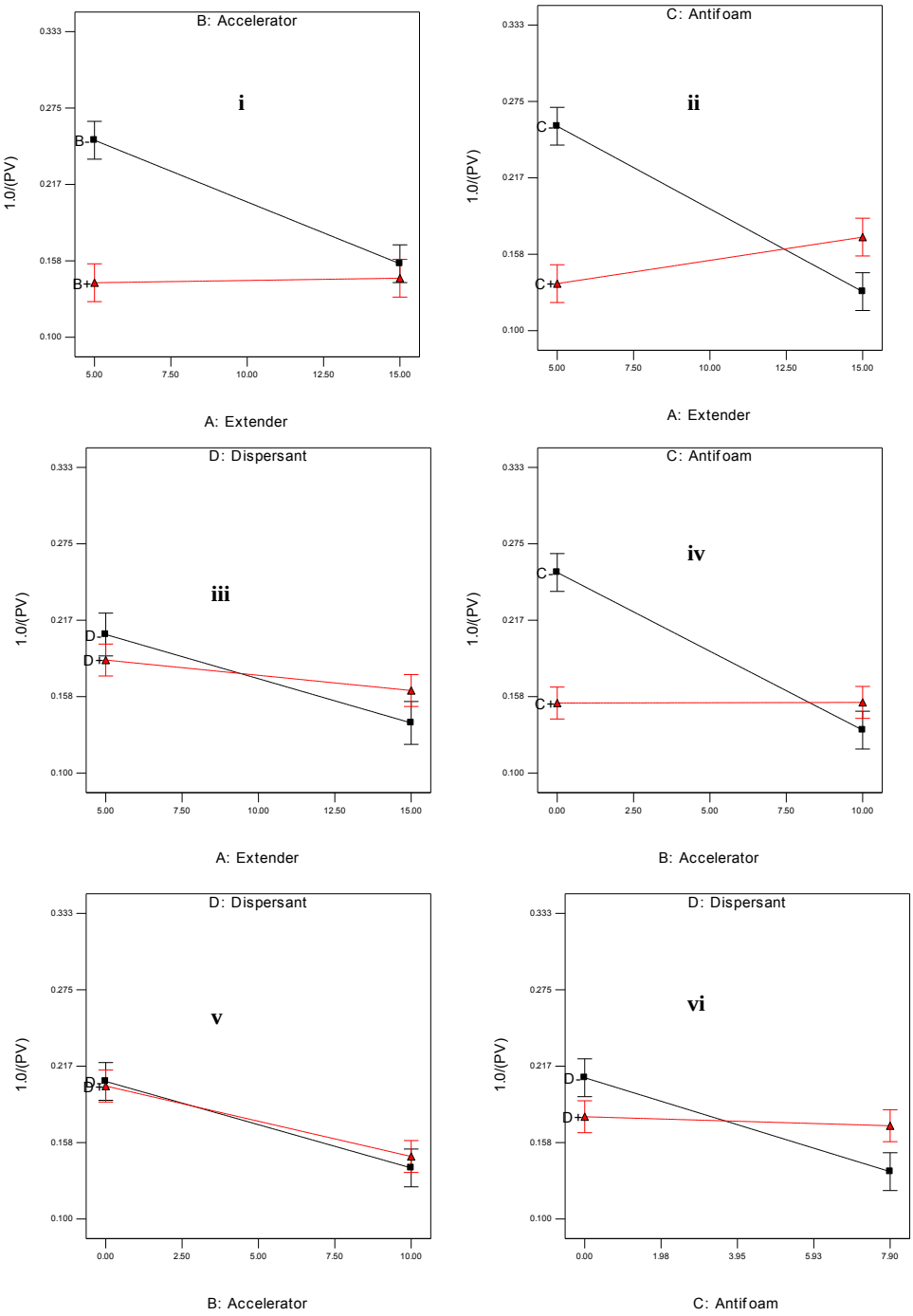

Fig 5: Effect of variables interactions on PV

Figure 4(ii) show that the relationship between the plastic viscosity and accelerator has an inverse relationship with constant percentages of extender, antifoam and dispersant respectively. There was a decrease in values of plastic viscosity from 0.203 to 0.143 when

the percentage of accelerator was increased from 0 to 10%. Presented in Figure 4(iii) was also an inverse relationship between plastic viscosity and antifoam at constant extender, accelerator and dispersant. There was a decrease in the value of plastic viscosity of class G cement slurry from 0.193 to 0.154 when the percentage of antifoam was varied from 0 to 7.9. Figure 4(iv) show a proportional relationship between the plastic viscosity and dispersant at constant extender, accelerator and antifoam. There was an increase in the value of plastic viscosity from 0.172 to 0.175 when the dispersant percentage was increased from 0 to 4.2%.

Shown in Figure 5(i-vi) are different combinations and effects of combining two variables and keeping other variables constant on plastic viscosity. Figure 5(i) show the effect of low and high values of accelerator with increase in extender percent from 5 to 15% at constant antifoam and dispersant. It was observed that at a low value of accelerator, the plastic viscosity decreased from 0.250397 to 0.156151 and increasing the value of accelerator to 10, the plastic viscosity slightly increased from 0.141617 to 0.145089 when the extender value was increased from 5 to 15%. The effect of simultaneous increase in value of extender and antifoam on plastic viscosity at constant accelerator and dispersant. It was noticed that increase in extender from 5 to 15% led to decrease in plastic viscosity from 0.256101 to 0.156151 at a low antifoam value and at a high antifoam value of 7.9%, the plastic viscosity increased from 0.135913 to 0.171429 when the extender value was increased from 5 to 15%. Different behavior was noticed for different combinations of two factors variables of extender and dispersant, accelerator and antifoam, accelerator and dispersant and antifoam and dispersant which are all pictorially represented in Figure 5(iii-vi).

Figure 6(i-vi) described the surface behavior of combination of variables on response variable. Figure (6i) show the 3D view of surface interaction between extender and accelerator at constant antifoam and dispersant. The surface plot show that plastic viscosity decreased from 0.250397 to 0.156151 when the extender value was increased, increase in antifoam value to 7.9 led to decrease in plastic viscosity given a minimum value of 0.141617 at extender value of 5% and further increase in extender value led to slightly increased in the plastic viscosity with a value of 0.145089 at 15%. The 3D surface interaction of extender and antifoam at constant accelerator and dispersant. It was observed that at low value of antifoam and extender highest value of plastic viscosity was recorder as 0.256101. Increase in value of antifoam decreased the value of plastic viscosity from 0.256101 to 0.135913, at a minimum value of extender but increased in extender value at high antifoam percent increased the value of plastic viscosity from 0.135913 to 0.171429. Surface interaction of extender and dispersant at constant accelerator and antifoam was shown in Figure 6(iii). It was observed from the plot that at a low dispersant value, a very high value of plastic viscosity of 0.205575 was recorded at extender value of 5% but increase in the extender value drastically reduced plastic viscosity value to 0.138244 at 15% while the high value of dispersant led to decreased in plastic viscosity value from 0.18626 to 0.162996 when extender value was increased from 5 to 15%. Increase in the value of extender lead to a corresponding reduction in the value of plastic viscosity from 0.205575 to 0.162996. 3D plot for accelerator - antifoam, accelerator - dispersant and antifoam - dispersant were all presented in Figure 6(iv-vi).

3.1.3 Interaction of variables on yield point

Figure 7(i-iv) described the individual behavior of the four factors used for the prediction of yield point. Figure 7(i) show that at constant accelerator of 5%, antifoam of 3.95% and dispersant of 2.10%; the relationship between the yield point and extender was a proportional relationship. There was a decrease in the value of yield point from 23 to 19.5 when the percentage of extender was increased from 5 to 15%.

Figure 7(ii) described that the relationship between the yield point and accelerator as a proportional relationship with constant percentages of extender 10, antifoam 3.95 and dispersant of 2.10% respectively. There was an increase in values of yield point from 20.9375 to 21.5625 when the percentage of accelerator was increased from 0 to 10%. Presented in Figure 7(iii) was the inverse relationship between yield point and antifoam at constant extender,

accelerator and dispersant. There was a decrease in value of yield point of class G cement slurry from 22 to 20.5 when the percentage of antifoam was varied from 0 to 7.9. Figure 7(iv) also shows the proportional relationship between the yield point and dispersant at constant extender, accelerator and antifoam. There was an increase in the value of yield point from 18.625 to 23.875 when the dispersant percentage was increased from 0 to 4.2%.

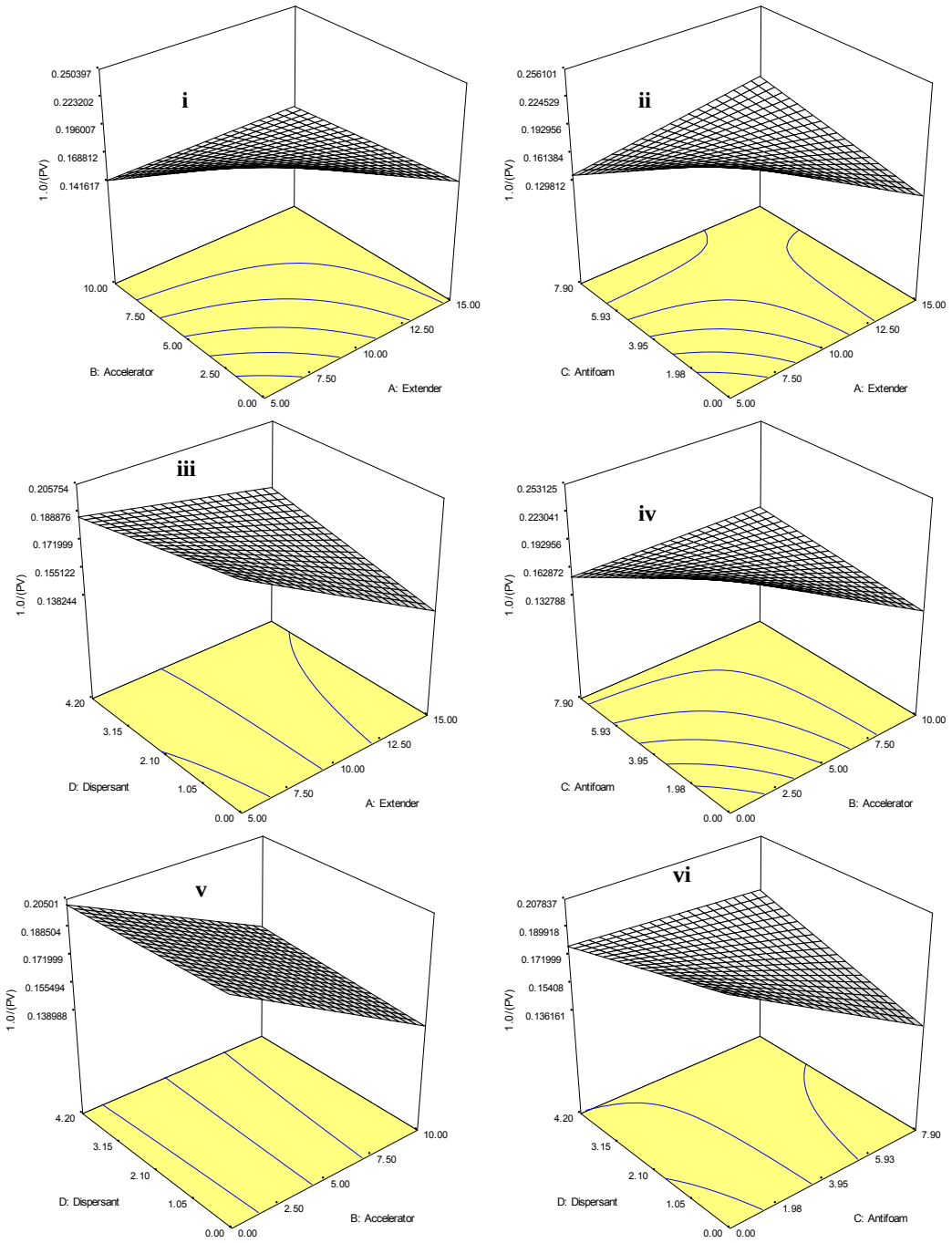

Fig 6: Surface plot of interactions of variables against PV

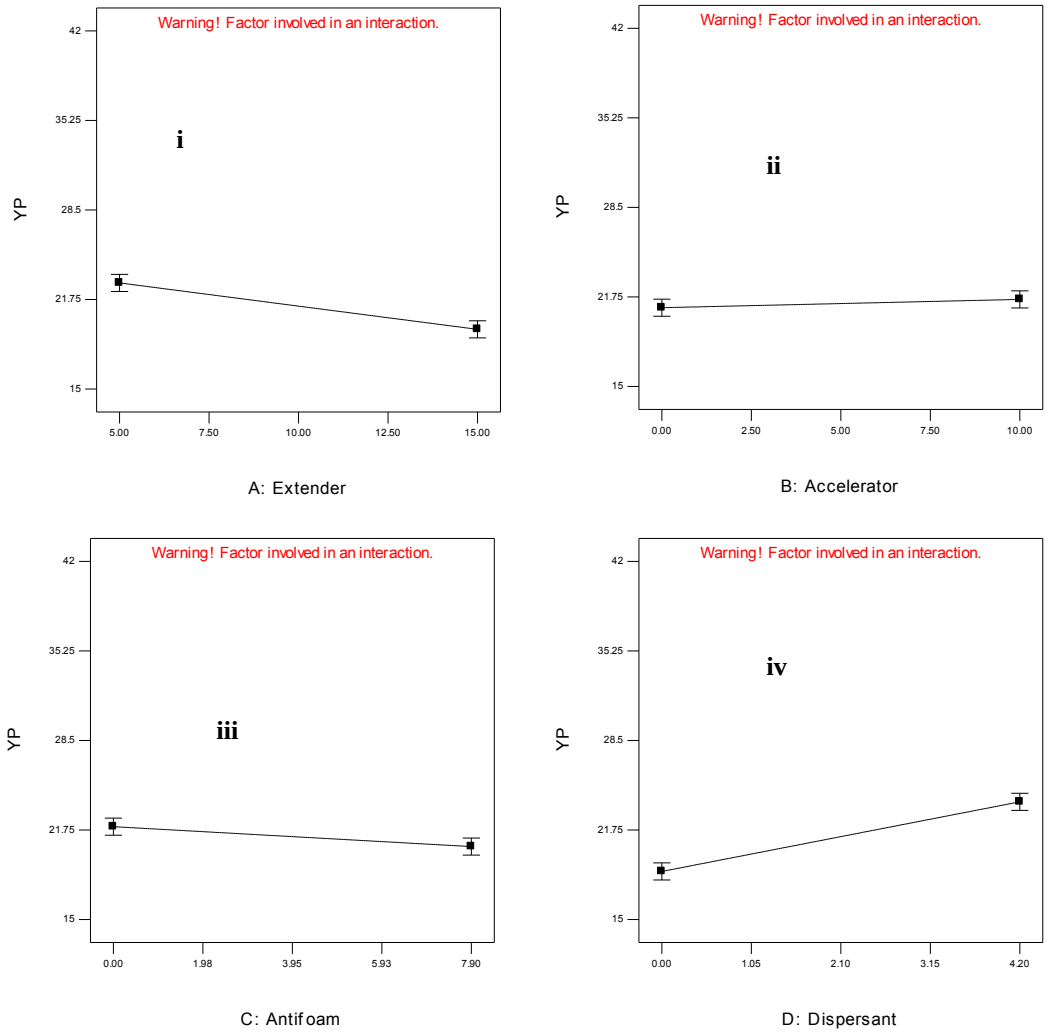

Fig 7: Effect of each variable on YP

Shown in Figure 8(i-vi) are different combinations and effects of combining two variables and keeping other variables constant on yield point. Figure 8 (i) show the effect of low and high values of accelerator with increase in extender percent from 5 to 15% at constant antifoam and disper-sant. It was observed that at a low value of accelerator, the yield point decreased from 21.625 to 20.25 when extender value was increased from 5 to 15%, and increasing the value of accelerator to 10, the yield point decreased from 24.375 to 18.75 when the extender value was increased from 5 to 15%. The effect of simultaneous increase in value of extender and antifoam on yield point at constant accelerator and dispersant. It was noticed that increase in extender from 5 to 15% led to decrease in yield point from 25.125 to 18.875 at a low antifoam value and at a high antifoam value of 7.9%, the yield point slightly decreased from 20.875 to 20.125 when the extender value was increased from 5 to 15%. Different behavior was noticed for different combinations of two factors variables of extender and dispersant, accelerator and antifoam, accelerator and dispersant and antifoam and dispersant which are all pictorially represented in Figure 8 (iii-vi).

Figure 9(i-vi) described the surface behavior of combination of variables on response variable. Figure 9i show the 3D view of surface interaction between extender and accelerator at constant antifoam and dispersant. The surface plot show that yield point decreased from 21.625 to

20.25 when the extender value was increased, increase in accelerator value from 0 to 10% led to increase in yield point given a maximum value of 24.375 at extender value of 5% and further increase in extender value led to decreased in the yield point with a value of 18.75 at 15%.

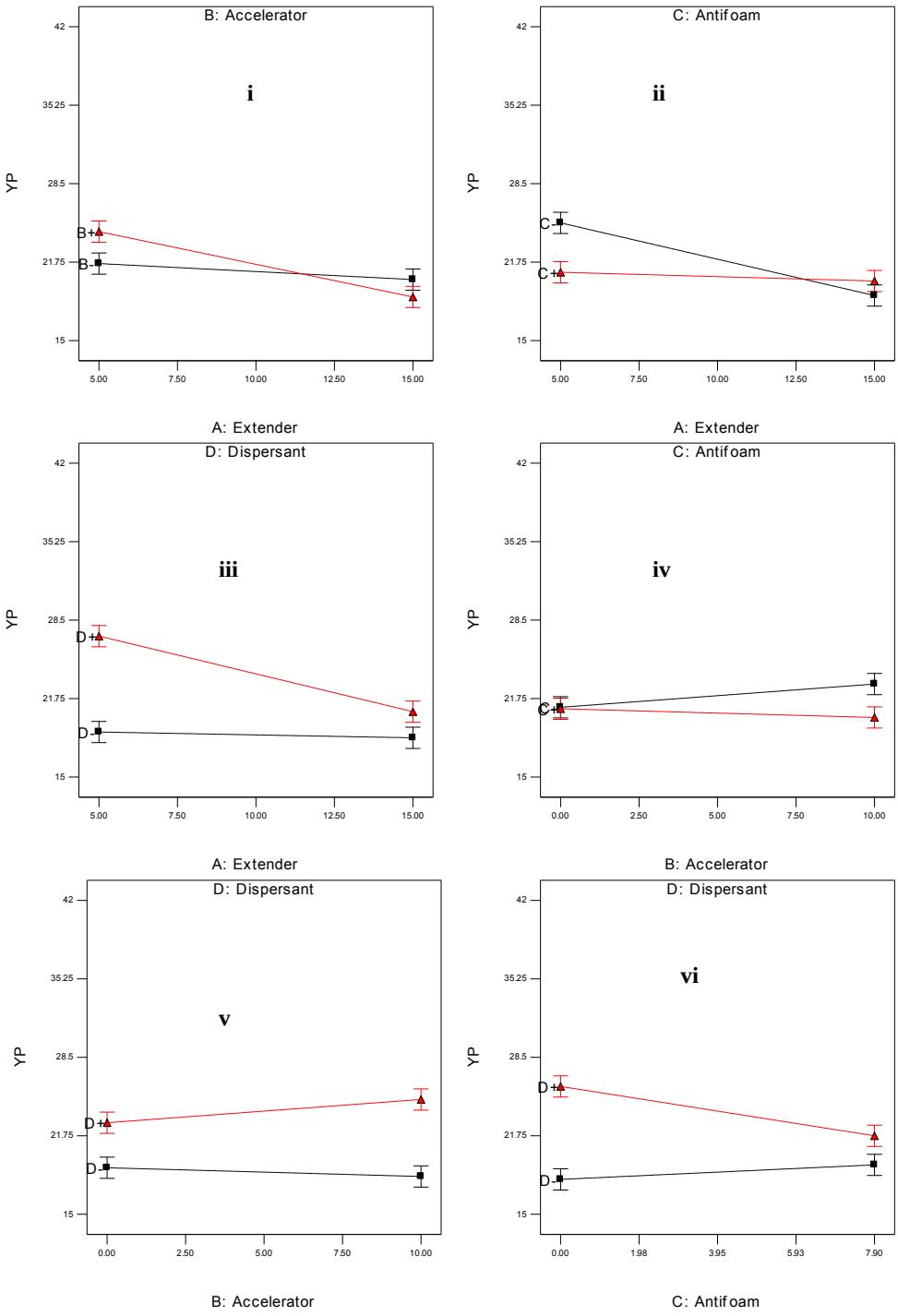

Fig 8: Effect of variables interaction on YP

The 3D surface interaction of extender and antifoam at constant accelerator and dispersant.

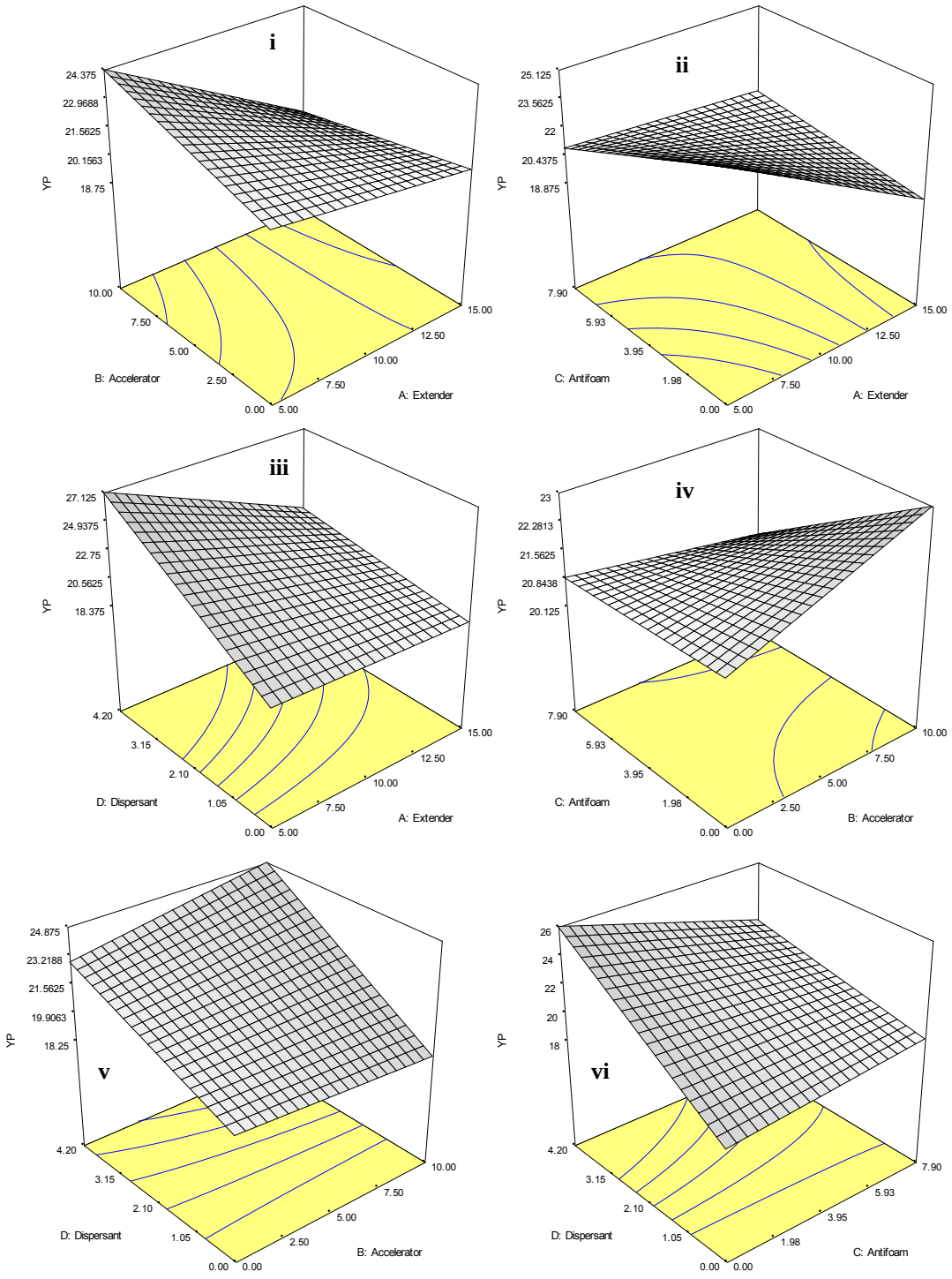

Fig 9: Surface plot of variables interaction on YP

It was observed that at low value of accelerator, highest value of yield point was recorded as 25.125 at a low value of antifoam. Increase in value of antifoam decreased the value of yield

point to 20.875 at a low value of extender but increased in extender value at high antifoam percent tend to have a detrimental effect on yield point increment with a value reduction from 20.875 to 20.125 at high value of extender. Surface interaction of extender and dispersant at constant accelerator and antifoam was shown in Figure 9(iii). It was observed that there was increased in value of yield point from 18.875 to 27.125 at low value of dispersant. Increase in value of dispersant from low to high value led to decrease in yield point value from 27.125 to 20.625 and similar trend was noticed when at high value of dispersant, there was a slight reduction in the value of yield point value from 18.875 to 18.375. 3D plot for accelerator - antifoam, accelerator - dispersant and antifoam - dispersant were all presented in Figure 4(iv-vi).

3.2 Validation of developed model

The experimental and the predicted result of the rheological parameter under investigation (PV, AV and YP) was presented on crossplot in Figure 10 and summarized in tabled in 4. The crossplot of the model developed for AV was shown in fig. 10i and was validated by analysing the value of correlation coefficient (R^2), adjusted R^2, Predicted R^2, standard deviation and Coefficient of Variance. The R-square value of the model gave 0.9940; the predicted R square gave a value of 0.9880 which was in agreement with adjusted R square value of 0.9724. Also there was agreement between the experimental and predicted values by the standard deviation of 0.39, coefficient of variance of 2.29 and Adequate prediction of 49.890 which are tabulated in Table 4.

Figure 10(ii) show the crossplot of the model developed for PV which was also validated by analysing the value of correlation coefficient (R^2), adjusted R^2, Predicted R^2, standard deviation and Coefficient of Variance. The R-square value of the model gave 0.9543; the predicted R square gave a value of 0.7879 which was in agreement with adjusted R square value of 0.9085. Also there was agreement between the experimental and predicted values by the standard deviation of 0.017, coefficient of variance of 10.92 and adequate prediction of 17.457.

The experimental result of yield point was plotted against predicted results on a bar chart in Figure 10(iii).

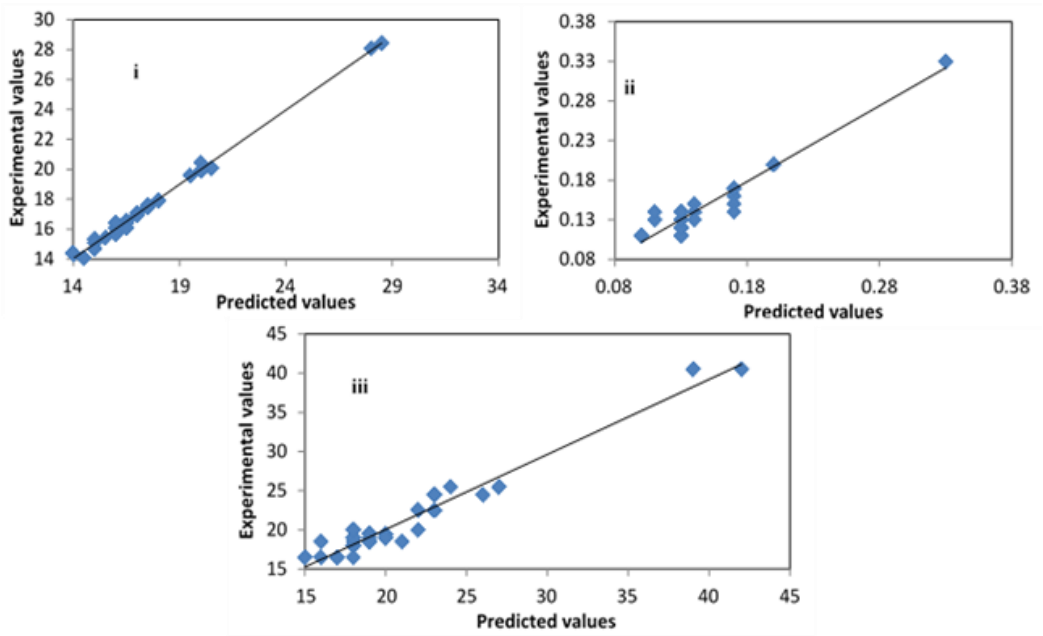

Fig 10: Crossplot of experimental versus predicted values for AV, PV and YP

The accuracy of the model developed was validated by analyzing the value of correlation coefficient (R^2), adjusted R^2, Predicted R^2, standard deviation and Coefficient of Variance. The R-square value of the model gave 0.9574; the predicted R square gave a value of 0.8060 which was in agreement with adjusted R square value of 0.9147. Also the was agreement between the experimental and predicted values by the standard deviation of 1.17, coefficient of variance of 8.06 and Adequate prediction of 19.226. The standard errors of the developed models are 0.098, 0.00437 and 0.3 for AV, PV and YP respectively.

Table 4 Statistical parameters of the model developed

Parameters	AV	PV	YP
R-Squared	0.993987049	0.954269265	0.9574
Adj R-Squared	0.987974098	0.90853853	0.9147
Pred R-Squared	0.972389511	0.787852684	0.806
Adequate Precision	49.8902642	17.45709181	19.226
Standard Deviation	0.393397896	0.017478494	1.71
Coeficient of Variance	2.29163823	10.91593688	8.06

3.3 ANOVA and statistical significance sf the model

The competence and significance of the model was justified by analysis of variance (ANOVA). The ANOVA for the model for prediction of rheological parameters (AV,PV & YP) was tabulated in table 5. The Model F-value of 20.87 implies the model is significant with a low chance that a "Model F-Value" this large could occur due to noise. Values of "Prob > F" less than 0.0500 in the model of PV model terms are significant. A, B, C, AB, AC, AD, BC, CD, ABC are significant model terms.

The ANOVA for the model for prediction of apparent viscosity was in Table 5.

Table 5 Analysis of variance(ANOVA) of the three rheological parameters

	Apparent Viscosity (AV)			Plastic Viscosity (PV)			Yield Point (YP)		
Factors	Mean Square	F Value	Prob > F	Mean Square	F Value	Prob > F	Mean Square	F Value	Prob > F
Model	25.583333	165.30769	< 0.0001	0.0063749	20.867132	< 0.0001	65.87	22.45	< 0.0001
A	19.140625	123.67788	< 0.0001	0.0082399	26.971997	0.0002	98	33.41	< 0.0001
B	49	316.61538	< 0.0001	0.0143619	47.011572	< 0.0001	3.13	1.07	0.3184
C	8.265625	53.408654	< 0.0001	0.0061735	20.207904	0.0006	18	6.14	0.0256
D	92.640625	598.60096	< 0.0001	2.765E-05	0.0904946	0.7683	220.5	75.17	<0.0001
AB	52.5625	339.63462	< 0.0001	0.0095489	31.256718	< 0.0001	36.13	12.32	0.0032
AC	28.890625	186.67788	< 0.0001	0.026181	85.699607	< 0.0001	60.5	20.62	0.0004
AD	83.265625	538.02404	< 0.0001	0.0019577	6.4082674	0.0251	72	24.55	0.0002
BC	110.25	712.38462	< 0.0001	0.0146007	47.793131	< 0.0001	15.13	5.16	0.0383
BD	14.0625	90.865385	< 0.0001	0.0001489	0.4873951	0.4974	15.13	5.16	0.0383
CD	97.515625	630.10096	< 0.0001	0.0041967	13.73717	0.0026	60.5	20.63	0.0004
ABC	156.25	1009.6154	< 0.0001	0.0097437	31.894593	< 0.0001	171.13	58.34	< 0.0001
ABD	3.0625	19.788462	0.0006	6.299E-05	0.2061821	0.6573	36.13	12.32	0.0032
ACD	43.890625	283.60096	< 0.0001				24.5	8.35	0.0112
BCD	14.0625	90.865385	< 0.0001	0.0004056	1.327587	0.2700	21.13	7.2	0.017
ABCD							136.12	46.41	< 0.0001

The Model F-value of 165.31 implies the model was significant with a low chance that a "Model F-Value" this large could occur due to noise. Values of "Prob > F" less than 0.0500 indicate model terms are significant. A, B, C, D, AB, AC, AD, BC, BD, CD, ABC, ABD, ACD, BCD are significant model terms.

The ANOVA for the model for prediction of yield point was in Table 5. The Model F-value of 22.45 implies the model is significant with a low chance that a "Model F-Value" this large could occur due to noise. Values of "Prob > F" less than 0.0500 indicate model terms are significant. A, C, D, AB, AC, AD, BC, BD, CD, ABC, ABD, ACD, BCD, ABCD are significant model terms.

3.4 Optimization studies

The numerical optimization was performed to maximize both PV and AV and minimize YP for selected range of variables A, B, C and D as 5 – 15%, 0 - 10, 0 – 7.9 and 0 – 4.2% respectively. By applying the desirability function method in Design Expert software, forty solutions were obtained for the optimum covering criteria with desirability value of 0.938 which is close to 1. In this case, first solution was selected as good desirability for which the optimized values of the responses are: PV, AV and YP values of 7.95, 21.44 and 26.88 subject to the values of A as 10.54, B as 10, C as 0.09 and D as 4.2% respectively.

4. Conclusion

A regression model was successfully developed for the determination of plastic viscosity, apparent viscosity and yield point for class G cement slurry. The addition of four different additives either individually or in different proportion triggered different behavior to the rheological parameters investigated. The most influencing parameter for plastic viscosity was combined interaction of AC, apparent viscosity was combined effect of ABC and yield point was D respectively. There was a close agreement between the result gotten from the model developed and experimental result gotten from the laboratory with their correlation coefficient and predicted correlation coefficient as 0.9939 and 0.9879 for AV, 0.9543 and 0.9085 for PV and 0.9574 and 0.9147 for yield point respectively. The optimization analysis show that in order to maximize PV and AV to 7.95 and 21.44 and then minimize YP to 26.88 the four variables must satisfy the values of A to be 10.54, B to be 10, C to be 0.09 and D to be 4.2.

References

[1] Roni G, Cristiane M, Kleber, T, Andre LM, Alex W. On the rheological parameter governing oil well cement slurry stability, Annual Transaction of the Nordic Rheology Society 2004, 12: 85-91.

[2] Boškovic Z, Cebašek V, Gojkovic N. Aplication of local cement for cementing oil wells in the south eastern region of the pannonian basin, Archives for Technical Sciences 2013, 8(1): 35-39.

[3] Thiercelin, MJ, Dargaurd B, Baret JF. and Rodriguez, W.J.: Cement design based on cement mechanical response, SPE Drilling and Completion December 1998: 266-273.

[4] Anjuman S, Moncef N. Modeling rheological properties of oil well cement slurries using multiple regression analysis and artificial neural networks, International Journal of Material Science (IJMSCI) 2013, 3(1): 26-37.

[5] Arild S, Jack OH and Erik J. The effect of gypsum and anhydrite on rheological properties of cement slurries, Annual Transaction of the Nordic Rheology Society 1994, 2: 85-87.

[6] Helge, H, Arid S. and Skule S. Rheological properties of high temperature oil well cement slurries, Annual Transaction of the Nordic Rheology Society 2001, 9: 1-8.

[7] Gonet A, Stryczek S and Pinka J. Analysis of rheological models of selected cement slurries, Acta Montanistica Slovaca 2004, 9(1): 16-20.
[8] Gintautas S, Mindaugas D, Arminas S. and Rimantas L. The influence of cement particles shape and concentration on the rheological properties of cement slurry, Materials Science 2005, 11(2): 150 – 158.
[9] Ershadi V, Ebadi T, Rabani AR, Ershadi L, Soltanian H. The Effect of Nanosilica on Cement Matrix Permeability in Oil Well to Decrease the Pollution of Receptive Environment. International Journal of Environmental Science and Development 2011, 2(2): 1-5.
[10] Pattinasarany A and Irawan S. The novel method to estimate effect of cement slurry consistency toward friction pressure in oil/gas well cementing, Research Journal of Applied Sciences, Engineering and Technology 2012, 4(22): 4596-4606.
[11] Dale PB, Ferraris CF, Galler MA, Hansen AS, Guynn JM. Influence of particle size distributions on yield stress and viscosity of cement-fly ash pastes, Cement and Concrete Research 2012, 42(2): 404-409.
[12] Salehi R and Paiaman AM. A novel cement slurry design applicable to horizontal well conditions, Petroleum & Coal 2009, 51(4): 270-276.
[13] Cheong Y, and Gupta R. Experimental design and analysis methods of assessing volumetric uncertainties. SPE Journal 2005: 9–11.
[14] Salam KK, Arinkoola AO, Oke EO, and Adeleye JO. Optimization of operating parameters using response surface methodology for paraffin-wax deposition in pipeline. Petroleum and Coal 2014, 56(1): 19-27.
[15] Kelechukwu EM, Hikmat SA and Yassin AM. Influencing factors governing paraffin wax deposition during crude production, International Journal of Physical Sciences 2010, 5(15): 2351-2362.
[16] Falode AO, Salam KK, Arinkoola AO, and Ajagbe BM. Prediction of compressive strength of oil field class G cement slurry using factorial design. Journal of Petroleum Exploration and Production Technology 2013, 3: 297-302.
[17] Salam KK, Arinkoola AO, Ajagbe B and Sanni O. Evaluation of thickening time of oil field class G cement slurry at high temperature and pressure using experimental design. International Journal of Engineering Science 2013, 2(8): 361-367.
[18] American Petroleum Institute. API Recommended Practice 10A: Specification for Cements and Materials for Well Cementing 2002, Washington, D.C.: 95-112.
[19] Adeleye JO, Salam KK and Adetunde IA. Analysis of rheological properties of treated Nigerian clay using factorial design, European Journal of Scientific Research 2009, 37(3):426–438.